Research Paper

Journal of Chemical Research

Journal of Chemical Research
1–6

DOI: 10.1177/1747519819890561
journals.sagepub.com/home/chl
SAGE

A novel coumarin-derived dithioacetal chemosensor for trace detection of Hg^{2+} in real water samples

Xing Ke[1], Yilei Fan[1,2], Jing Zhou[1] and Zhongping Huang[3]

Abstract

A novel coumarin-derived dithioacetal chemosensor, 8-(1,3-dithian-2-yl)-7-hydroxy-4-methylcoumarin (**LS**), has been designed and synthesized. The sensor **LS** showed highly selective fluorescent sensing for Hg^{2+} with a low detection limit of 0.81 nM in the pH range from 6.15 to 9.96 in ethanol/water (1:1, v/v) solution. The sensing mechanism of **LS** toward Hg^{2+} was proposed and verified by ^1H nuclear magnetic resonance spectroscopy studies. Under an ultraviolet lamp, the fluorescence color changes could be easily detected by the naked eye. In addition, the sensor **LS** has been applied in the trace detection of Hg^{2+} in real water samples.

Keywords

chemosensor, coumarin, desulfurization, dithioacetal, mercury(II) ions

Date received: 12 August 2019; accepted: 1 November 2019

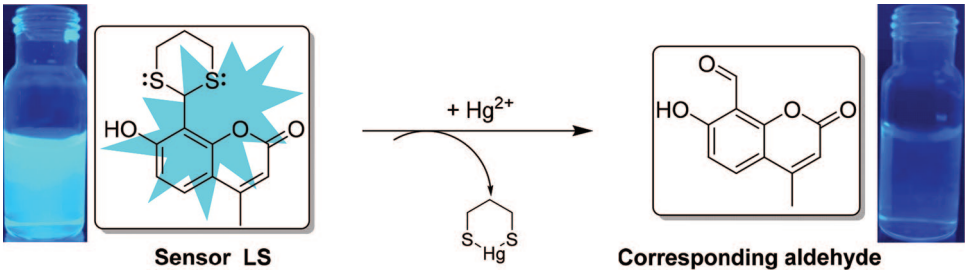

Introduction

Mercury is a natural component of our environment; it constitutes 0.5 parts per million of the Earth's crust and is one of the most toxic metals.[1] Mercury species are broadly classified into three different chemical categories (elemental forms, divalent inorganic forms, and organic mercury), which have different toxic-kinetic properties.[2] Hg^{2+} (inorganic form) is highly soluble, is the most stable form of inorganic mercury in the aquatic environment; it is carcinogenic and displays high cellular toxicity.[3] The WTO explicitly defined that the concentration of Hg^{2+} in drinking water must be less than $6\,\mu g\,L^{-1}$ (30 nM).[4] Mercury can be absorbed by microorganisms and converted into methylmercury, which can enter into the food chain and cause various grave disorders and illness. Long-lasting uptake of high levels of mercury can lead to serious health problems, such as neurological damage, effects on the immune system, Minamata disease, muscle weakness, motion disorders, and chronic diseases.[5–7] Therefore, the development of methods for efficiently detecting Hg^{2+} is of great significance.

In the last few decades, significant efforts have been made to quantify mercury species, and many methods have been reported, such as atomic absorption-emission spectroscopy,[8] polarography,[9] reversed-phase high-performance

[1]Key Laboratory of Drug Prevention and Control Technology of Zhejiang Province, Department of Criminal Science and Technology, Zhejiang Police College, Hangzhou, P.R. China
[2]College of Pharmaceutical Science & Green Pharmaceutical Collaborative Innovation Center of Yangtze River Delta Region, Zhejiang University of Technology, Hangzhou, P.R. China
[3]College of Chemical Engineering, Zhejiang University of Technology, Hangzhou, P.R. China

Corresponding author:
Yilei Fan, Key Laboratory of Drug Prevention and Control Technology of Zhejiang Province, Department of Criminal Science and Technology, Zhejiang Police College, Hangzhou 310053, P.R. China.
Email: fanyilei@zjjcxy.cn

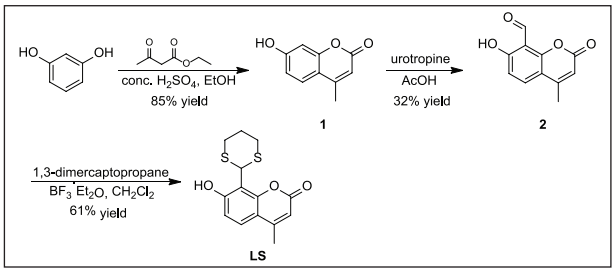

Scheme 1. Synthetic protocol for sensor **LS.**

liquid chromatography,[10] and infrared spectroscopy.[11,12] Unfortunately, most of these methods are not appropriate for real-time and on-site assays and require expensive devices and complicated sample preparation. In recent years, chemosensors for detecting mercury ions have attracted great attention due to their high selectivity and excellent sensitivity. In addition, fluorescent chemosensors which can directly measure mercury ions in water samples are advantageous in terms of time savings, lower costs, and simplicity.[13]

There are two types of fluorescent chemosensors for Hg^{2+} detection that have been reported: coordination-based chemosensors[14–16] and reaction-based chemosensors.[17–26] For reaction-based sensors, the determination of Hg^{2+} is achieved by specific chemical reactions between receptors and Hg^{2+}. This type of chemosensor usually exhibits excellent selectivity and high sensitivity toward Hg^{2+} due to their specific selective reactivity to Hg^{2+}.[13] Therefore, research of reaction-based chemosensors has gained more attention in recent years.

With large molar extinction coefficients, relatively long excitation and emission wavelengths and high quantum efficiencies, coumarin derivatives have been widely used as fluorescent chemosensors.[27] It has been reported that the thioacetal group can be selectively desulfurized by Hg^{2+}, resulting in the formation of the corresponding aldehyde and changes of the fluorescent intensity. However, most of these chemosensors have drawbacks of relatively high fluorescent background signals, limits of detection,[28] and poor solubility in aqueous solution.[29] Herein, we have designed and synthesized a novel "on-off" fluorescent chemosensor, 8-(1,3-dithian-2-yl)-7-hydroxy-4-methylcoumarin (**LS**) (Scheme 1), in which a thioacetal group has been added to a coumarin derivative. The sensor **LS** showed highly selective fluorescent sensing for Hg^{2+} with a low detection limit of 0.81 nM in the pH range from 6.15 to 9.96 in ethanol/water (1:1, v/v) solution. The recognition mechanism of sensor **LS** toward Hg^{2+} is proposed and confirmed by ^1H nuclear magnetic resonance spectroscopy (NMR) studies.

Results and discussion

The ultraviolet–visible (UV–Vis) titration spectra of sensor **LS** upon addition of various concentrations of Hg^{2+} were carried out in ethanol and water (1:1, v/v) at room temperature. As shown in Figure 1, the absorption band of receptor **LS** in the UV–Vis spectrum appears at 272 nm. Upon addition of increasing concentrations of Hg^{2+} (0–0.75 equiv.) to the solution of sensor **LS** (100 μM), the absorption band at 272 nm was enhanced gradually, which clearly suggests that **LS** participates in a reaction with Hg^{2+}.

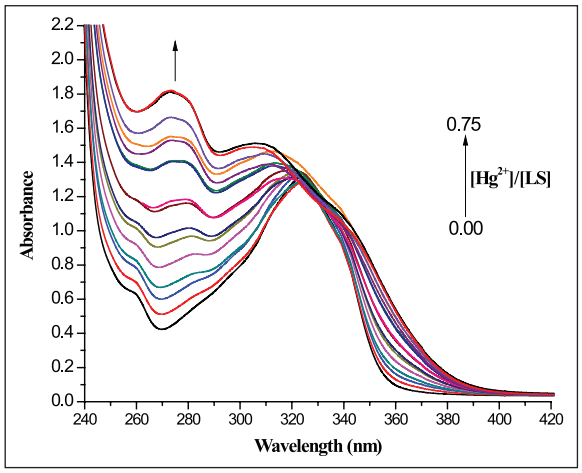

Figure 1. Absorption spectra of sensor **LS** (100 μM) in ethanol and water (1:1, v/v) solution obtained by adding aliquots of $[Hg^{2+}]$ (0, 0.05, 0.10, 0.15, 0.20, 0.25, 0.30, 0.35, 0.40, 0.45, 0.50, 0.55, 0.60, 0.65, 0.70, and 0.75 equiv.).

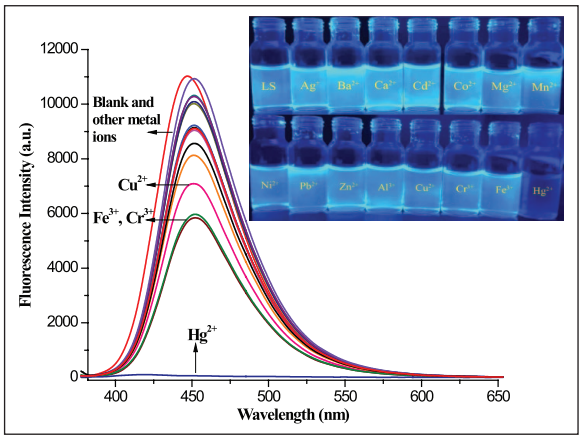

Figure 2. Fluorescent spectra of sensor **LS** (2 μM) with 1.0 equiv. of various metal ions in ethanol and water (1:1, v/v). Inset: The colors of sensor **LS** upon addition of various metal ions as viewed by the naked eye under a 365-nm UV lamp.

The fluorescence emissions of sensor **LS** (2 μM) on adding different metal ions (1.0 equiv. of **LS**) including Ag^{+}, Al^{3+}, Ba^{2+}, Ca^{2+}, Cd^{2+}, Co^{2+}, Cu^{2+}, Cr^{3+}, Fe^{3+}, Hg^{2+}, Mg^{2+}, Mn^{2+}, Ni^{2+}, Pb^{2+}, and Zn^{2+} were determined in ethanol/water (1:1, v/v). After excitation at 369 nm, the sensor **LS** exhibited very strong fluorescence emission at 451 nm. Upon the addition of Hg^{2+} (2 μM), the fluorescence intensity was quenched immediately (Figure 2). In contrast, no significant fluorescence change was detected after addition of other metal ions under the same conditions, except for with Cu^{2+}, Fe^{3+}, and Cr^{3+}. These common fluorescence-quenching ions (Cu^{2+}, Fe^{3+}, and Cr^{3+}) quenched about 23%–36% of the fluorescence compared with **LS** alone. Under the 365-nm UV lamp, the remarkable light-blue fluorescence emission of sensor **LS** disappeared after adding Hg^{2+}, but no significant fluorescence change was detected for **LS** solution with other metal ions. These results indicate that sensor **LS** exhibited high selectivity for Hg^{2+} over other metal ions.

The quantitative sensing abilities of sensor **LS** (2 μM) toward Hg^{2+} were studied and a working curve was obtained (Figure 3). With addition of increasing concentrations of

Hg^{2+} ions (0.2, 0.4, 0.6, 0.8, 1.0, 1.2, 1.4, 1.6, 1.8, 2.0, 2.2, 2.4, 2.6, 2.8, 3.0, 3.2, and 3.4 μM), the fluorescence intensity of **LS** at 451 nm decreased significantly. Besides, a good linear correlation ($R^2 = 0.9937$) between the emission intensity of **LS** and the concentration of Hg^{2+} was observed on addition of 0–1.0 equiv. of Hg^{2+} ions.

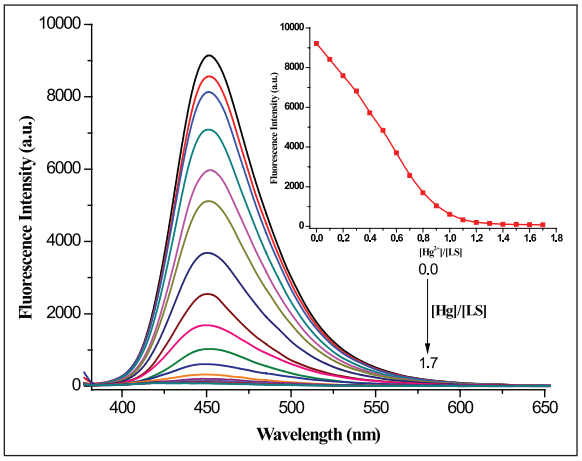

Figure 3. Fluorescence titrations of 2 μM **LS** ($\lambda_{ex} = 369$ nm) in ethanol and water (1:1, v/v) in the presence of different equivalents of Hg^{2+} ions (0, 0.1, 0.2, 0.3, 0.4, 0.5, 0.6, 0.7, 0.8, 0.9, 1.0, 1.1, 1.2, 1.3, 1.4, 1.5, 1.6, and 1.7 equiv.). Inset: Graph of the fluorescence intensity at 451 nm as a function of the concentration ratio of Hg^{2+} and **LS**.

According to the 3σ method (limit of detection (LOD) = 3σ/K, σ represents the standard deviation of a blank solution and K represents the slope of the calibration curve in Supplemental Figure S1), the LOD of chemosensor **LS** for Hg^{2+} reached 0.81 nM, which is much lower for the detection of Hg^{2+} than other published Hg^{2+} chemosensors (Table 1).[30–37] These results demonstrate that sensor **LS** could be potentially used for selective detection of trace amounts of Hg^{2+} in analytical chemistry.

To determine the utility of sensor **LS** (2 μM) as a Hg^{2+}-selective receptor in the complex background of competing species, the fluorescence emissions of **LS**-M solutions (M represents different metal ions, 1 equiv. of **LS**) were examined in the presence of Hg^{2+} (Figure 4). **LS**-M solutions exhibited strong fluorescence emissions, even with common fluorescence-quenching ions (such as Cu^{2+}, Cr^{3+}, and Fe^{3+}). Upon addition of Hg^{2+} (1 μM), the fluorescence emissions of the **LS**-M solutions were quenched almost immediately. This result demonstrated that sensor **LS** has the potential to efficiently detect Hg^{2+} in complex environments and is not interfered with other competing species.

The fluorescence emission time-course of sensor **LS** with Hg^{2+} in ethanol/water (1:1, v/v) was studied (see Supplemental Figure S2). After adding Hg^{2+} to the **LS** solution, the fluorescence emission of **LS**-Hg^{2+} was significantly decreased in 2 min. The minimum of fluorescence intensity of **LS**-Hg^{2+} was reached after 6 min and then remained stable. This result demonstrated that the

Table 1. Comparison of **LS**-Hg^{2+} sensing with other dithioacetal-based Hg^{2+} fluorescent sensors.

Sensor	$\lambda_{ex}/\lambda_{em}$ (nm)	Sensing method	Detection limit	pH tolerance
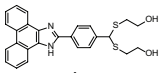	390/509	Fluorescence[31]	1.16×10^{-9} M	7.4
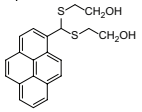	395/457	Fluorescence[32]	1.03×10^{-9} M	7.4
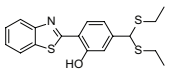	449/552	Fluorescence[33]	1.59×10^{-8} M	7.4
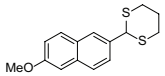	300/412	Fluorescence[34]	5.0×10^{-6} M	–[a]
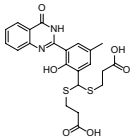	420/538	Fluorescence[35]	2.04×10^{-8} M	7–12
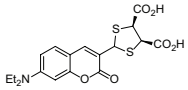	477/502	Colorimetric fluorescence[36]	2.4×10^{-8} M	7.4
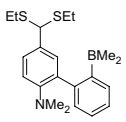	320/503	Fluorescence[37]	7.27×10^{-8} M	–[a]
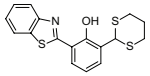	349/526	Fluorescence[38]	2.0×10^{-7} M	5.0–9.0
This work	369/451	Fluorescence	8.1×10^{-10} M	6.15–9.96

[a]Not mentioned.

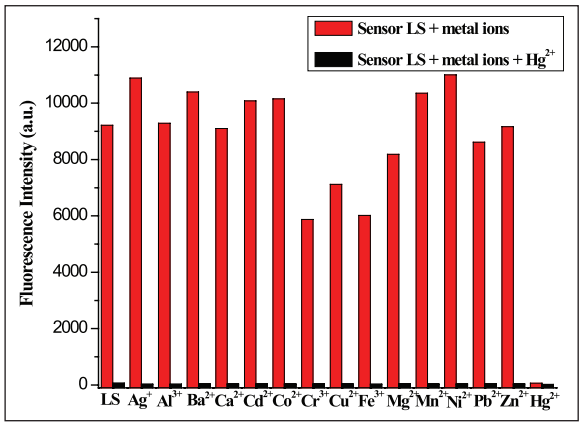

Figure 4. Fluorescence intensities of **LS**-M (2 μM) solutions in the absence and presence of Hg^{2+} (1 μM). (λ_{ex} = 369 nm, λ_{em} = 451 nm).

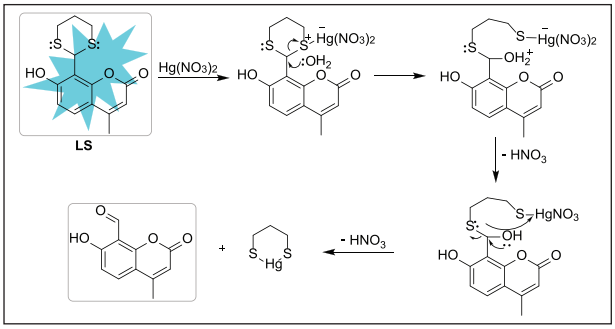

Scheme 2. Proposed sensing mechanism between sensor **LS** and Hg^{2+}.

reaction between **LS** and Hg^{2+} proceeded quickly, and sensor **LS** could be practically used for the practical and rapid detection of Hg^{2+}.

To investigate the applicability of sensor **LS** for detecting Hg^{2+} in different environments, the pH effects were studied (see Supplemental Figure S3). The fluorescence emissions of **LS** (2 μM) in the absence and presence of Hg^{2+}(2 μM) were detected in various buffer solutions (see Supplemental Table S1). The free sensor **LS** exhibited relatively strong fluorescence emissions in the pH range of 6.15–9.96. Upon addition of Hg^{2+}, the fluorescence emissions of the resulting solutions were quenched efficiently. These results demonstrated that sensor **LS** was highly sensitive toward Hg^{2+} in a relatively wide pH range (6.15–9.96). Considering that major biological imaging experiments are performed in neutral environments, sensor **LS** could be suitable for measuring Hg^{2+} in biological samples.

Based on the above results, a proposed Hg^{2+}-promoted hydrolysis desulfurization mechanism for the fluorescence response of **LS** toward Hg^{2+} is proposed. As shown in Scheme 2, sensor **LS** emits strong light-blue fluorescent emission. Upon addition of Hg^{2+} to the solution of **LS**, the coordination between $Hg(NO_3)_2$ and the sulfur atom of **LS** caused activation of the carbon atom on thioacetal. The resulting activated carbon atom is then attacked by a water molecule to afford the corresponding aldehyde.

Additional evidence was given by NMR studies of the **LS** and **LS**-Hg^{2+} mixture. The ^{1}H NMR spectra of **LS** in the absence and presence of Hg^{2+} were recorded in $CDCl_3$. Significant spectral changes were observed (Figure 5). Signals for the protons of the methylene (3.16, 2.91, 2.23, and 1.93 ppm) and methine groups (6.26 ppm) disappeared in the presence of Hg^{2+}, and a new resonance at 10.62 ppm formed being characteristic of an aldehyde proton. These phenomena indicated that the reaction between Hg^{2+} and **LS** causes desulfurization and formation of the corresponding aldehyde.

By utilizing a previously reported method,[38,39] sensor **LS** was used to measure the Hg^{2+} content in actual water samples, including tap water (from our laboratory), domestic sewage (from student residences at our university), and industrial sewage (from industrial areas in Hangzhou City). All the water samples were filtered through a 0.2-mm filter membrane to remove large particular impurities, followed by the removal of remaining organics by extraction processes. The resulting samples were diluted with ethanol and water (1:1, v/v) in a 10.0-mL volumetric flask. Table 2 shows the results acquired using sensor **LS** with the appropriate concentration gradient of Hg^{2+} added. The results indicate that sensor **LS** had good recovery and demonstrated high accuracy in the analysis of Hg^{2+}. Therefore, sensor **LS** can measure the concentration of Hg^{2+} in real water samples and has practical value in the environmental analysis.

Conclusion

In summary, a highly selective and sensitive coumarin-derived dithioacetal chemosensor, 8-(1,3-dithian-2-yl)-7-hydroxy-4-methylcoumarin (**LS**), has been designed and synthesized. **LS** shows significant "on-off" fluorescence behavior with Hg^{2+} in ethanol/water (1:1, v/v) solution, with strong light-blue fluorescent emission quenching. The detection limit was calculated to be 8.1×10^{-10} mol L^{-1} and remained stable, detecting Hg^{2+} in the pH range of 6.15–9.96. In addition, the sensor **LS** exhibits satisfactory results for Hg^{2+} detection in the analysis of real water samples and can be further used in potential applications for the detection of nanomolar concentrations of Hg^{2+} in chemical and environmental systems.

Experimental

All chemicals and solvents were obtained from commercial sources and used without further purification, except when specified. Solvents used in fluorescent experiments were of spectroscopic grade. The ^{1}H NMR and ^{13}C NMR spectra of the ligand were recorded on an Agilent 400-MR DDR2 spectrometer. The chemical shifts (δ) are recorded in ppm, relative to tetramethylsilane ($SiMe_4$). The Fourier transform infrared spectrum was recorded on a Thermo-Nocilet IR200 spectrophotometer. Mass spectra were obtained using a Shimadzu LCMS-2020 spectrometer. A.Mapada UV-6100 UV–Vis spectrophotometer was used for recording the UV–Vis spectra. Fluorescence emission spectra were recorded on a Dual-FL fluorescence spectrophotometer. Elemental analysis (C, H, and N) was performed with

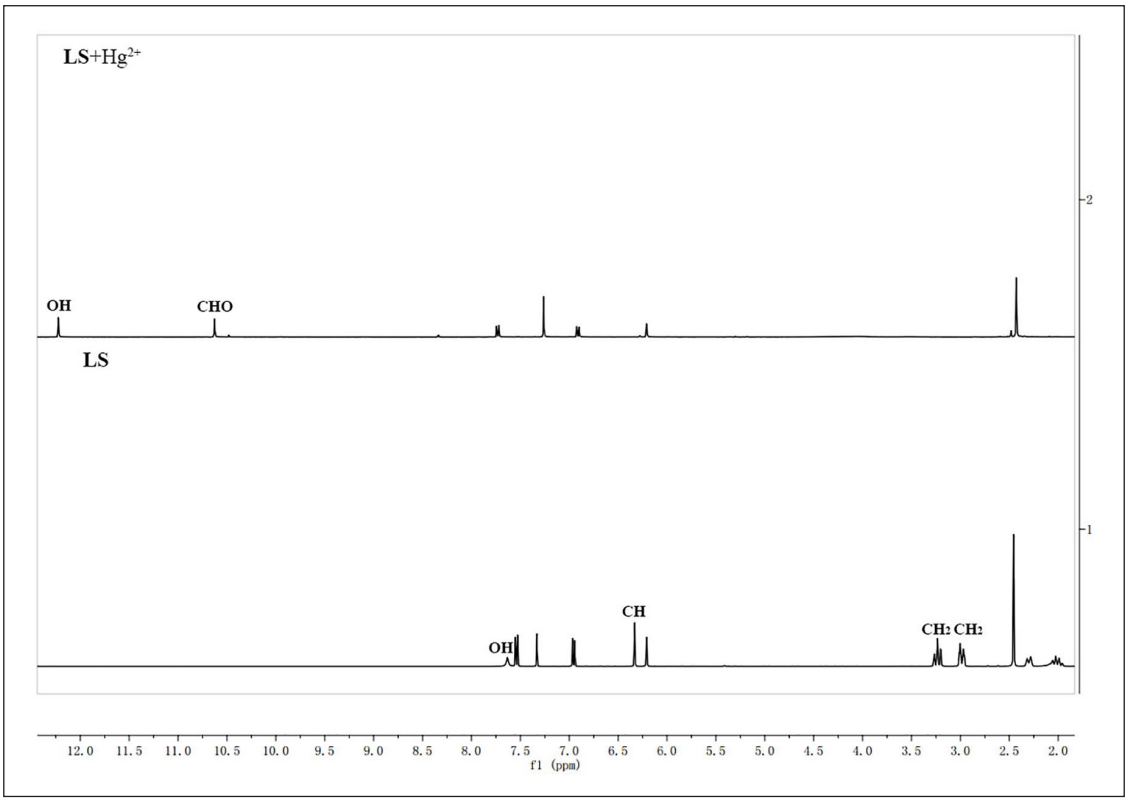

Figure 5. ^{1}H NMR spectra of sensor **LS** and **LS**-Hg^{2+} in $CDCl_3$.

Table 2. Determination of Hg^{2+} in real water samples with sensor **LS.**

Sample	pH[a]	Added Hg^{2+} (nM)	Found[b] Hg^{2+} (nM)	Recovery (%)	RSD (%)
Tap water	6.75	2	1.91	95.50	2.75
		4	3.93	98.25	
		6	6.06	101.00	
Domestic sewage	7.91	2	1.96	98.00	1.21
		4	3.99	99.75	
		6	6.02	100.33	
Industrial sewage	8.22	2	2.05	102.50	1.63
		4	3.97	99.25	
		6	6.04	100.67	

RSD: relative standard deviation.
[a]Determined with a pH meter before treating with Hg^{2+}.
[b]Results are based on three measurements.

an Elementar Vario MICRO cube and the results are within ±0.4% of the calculated values. All the solvents were purified before use. Compounds **1** and **2** (Scheme 1) were prepared starting from resorcinol according to a literature procedure.[40]

Preparation of 8-(1,3-dithian-2-yl)-7-hydroxy-4-methylcoumarin (sensor **LS***)*

To a solution of compound **2** (204 mg, 1 mmol) in dichloromethane (10 mL) was added 1,3-dimercaptopropane (108 mg, 1 mmol), followed by five drops of boron trifluoride-diethyl etherate. The mixture was then stirred at room temperature (25 °C) for 12 h. After completion of that reaction, the resulting mixture was made alkaline with saturated sodium bicarbonate to pH 8–9 and then extracted with dichloromethane (50 mL). The organic layer was separated, dried over anhydrous sodium sulfate, and then concentrated in vacuo. The crude product was purified by flash chromatography (petroleum/ethyl acetate = 2:1, v/v) to afford the desired product (179 mg) as white solid. Yield 61%. M.p. 203–204 °C. IR (KBr, cm^{-1}): 3310, 2919, 2891, 1712, 1607, 1572, 1392, 1362, 1317, 1064, 855, 809, 675. ^{1}H NMR (400 MHz, $CDCl_3$): δ = 7.56 (s, 1H), 7.47 (d, *J* = 8.8 Hz, 1H), 6.88 (d, *J* = 8.8 Hz, 1H), 6.26 (s, 1H), 6.14 (s, 1H), 3.13-3.20 (m, 2H), 2.89-2.94 (m, 2H), 2.39 (s, 3H), 2.20–2.26 (m, 1H), 1.92–1.99 (m, 1H). ^{13}C NMR (100 MHz, $CDCl_3$): δ = 160.74, 159.86, 153.10, 151.07, 125.88, 114.45, 113.21, 111.56, 110.96, 39.23, 31.20, 24.58, 18.85. MS (*m*/*z*): 316.95 $[M^{+}23]^{+}$. Anal. calcd for $C_{14}H_{14}O_3S_2$: C, 57.12; H, 4.79; S, 21.78; found: C, 57.15; H, 4.79; S, 21.79%.

Declaration of conflicting interests

The author(s) declared no potential conflicts of interest with respect to the research, authorship, and/or publication of this article.

Funding

The author(s) disclosed receipt of the following financial support for the research, authorship, and/or publication of this article: This work was supported by the National Key Research and Development Program of China (No. 2018YFC0807400) and the Analysis and Measurement Foundation of Zhejiang Province (No. LGC19B050003).

ORCID iD

Yilei Fan https://orcid.org/0000-0003-0737-9757

Supplementary material

Supplementary material is available online for this article.

References

1. Selin NE. *J Environ Monit* 2011; 13: 2389.
2. Henriques MC, Loureiro S, Fardilha M, et al. *Reprod Toxicol* 2019; 85: 93.
3. Faghiri F and Ghorbani F. *J Hazard Mater* 2019; 374: 329.
4. WHO. *The international programme on chemical safety. Environmental health criteria I. Mercury*. Geneva: World Health Organization, 1976.
5. Park H, Naveen M, An KL, et al. *J Nanosci Nanotechnol* 2019; 19: 6893.
6. Sharma BM, Sanka O, Kalina J, et al. *Environ Int* 2019; 125: 300.
7. Kim KH, Kabir E and Jahan SA. *J Hazard Mater* 2016; 306: 376.
8. Fong B, Mei W, Siu TS, et al. *J Anal Toxicol* 2007; 31: 281.
9. Mandil H, Sakur AA and Alulu S. *Asian J Chem* 2012; 24: 2980.
10. Wang L, Zhou JB, Wang X, Wang ZH and Zhao RS. *Anal Bioanal Chem* 2016; 408: 4445.
11. Zohar M, Auslender M, Faraone L, et al. *Opt Quantum Electron* 2012; 44: 95.
12. Chandrasoma A, Hamid AAA, Bruce AE, et al. *Anal Chim Acta* 2012; 728: 57.
13. Guo Y, An J, Tang HY, et al. *Mater Res Bull* 2015; 63: 155.
14. Wang H and Chan WH. *Tetrahedron* 2007; 63: 8825.
15. Fan JL, Guo KX, Peng XJ, et al. *Sens Actuators B* 2009; 142: 191.
16. Ho IT, Lai TL, Wu RT, et al. *Analyst* 2012; 137: 5770.
17. Qi Z and Tian H. *Sens Actuators B* 2010; 149: 20.
18. Cheng XH, Li S, Zhong AS, et al. *Sens Actuators B* 2011; 157: 57.
19. Kim JH, Kim HJ, Kim SH, et al. *Tetrahedron Lett* 2009; 50: 5958.
20. Lee DN, Kim GJ and Kim HJ. *Tetrahedron Lett* 2009; 50: 4766.
21. Wang F, Nam SW, Guo Z, et al. *Sens Actuators B* 2012; 161: 948.
22. Lee HY, Swamy KHK, Jung JY, et al. *Sens Actuators B* 2013; 182: 532.
23. Kaur M and Choi DH. *Sens Actuators B* 2014; 190: 542.
24. Prabhu J, Velmurugan K and Nandhakumar R. *J Lumin* 2014; 145: 733.
25. Kumari N, Dey N and Bhattacharya S. *Analyst* 2014; 139: 2370.
26. Wang G, Xu G, Zhu Y, et al. *Chem Commun* 2014; 50: 747.
27. Chen KY, Guo Y, Lu ZH, et al. *Chin J Chem* 2010; 28: 55.
28. Shinohara Y, Tsukamoto K and Maeda H. *J Photoch Photobiol A* 2019; 371: 407.
29. Cheng XH, Li QQ, Qin JG, et al. *ACS Appl Mater Interfaces* 2010; 2: 1066.
30. Gao Y, Yi N, Ou Z, et al. *Sens Actuators B* 2018; 267: 136.
31. Gao Y, Ma T, Ou Z, et al. *Talanta* 2018; 178: 663.
32. Zhou Y, He X, Chen H, et al. *Sens Actuators B* 2017; 247: 626.
33. Prabhu J, Velmurugan K and Nandhakumar R. *J Lumin* 2014; 145: 733.
34. Tang L, Ding S, Zhang X, et al. *J Photochem Photobiol A* 2017; 340: 15.
35. Xu QW, Wang C, Sun ZB, et al. *Org Biomol Chem* 2015; 13: 3032.
36. Song C, Yang W, Zhou N, et al. *Chem Commun* 2015; 51: 4443.
37. Chang IJ, Hwang KS and Chang SK. *Dyes Pigments* 2017; 137: 69.
38. Qu SZ, Zheng CH, Liao GM, et al. *RSC Adv* 2017; 7: 9833.
39. Wu X, Chen J and Zhao JX. *Analyst* 2013; 138: 5281.
40. Huang DD, Chen YH and Zhao JZ. *Dyes Pigments* 2012; 95: 732.